NASA Technical Memorandum 107070

Direct Numerical Simulation of Acoustic Waves Interacting With a Shock Wave in a Quasi-1D Convergent-Divergent Nozzle Using an Unstructured Finite Volume Algorithm

Trong T. Bui and Reda R. Mankbadi
Lewis Research Center
Cleveland, Ohio

Prepared for the
Joint Fluids Engineering Conference
cosponsored by the American Society of Mechanical Engineers
and the Japan Society of Mechanical Engineers
Hilton Head, South Carolina, August 13–18, 1995

National Aeronautics and
Space Administration

DIRECT NUMERICAL SIMULATION OF ACOUSTIC WAVES INTERACTING WITH A SHOCK WAVE IN A QUASI-1D CONVERGENT-DIVERGENT NOZZLE USING AN UNSTRUCTURED FINITE VOLUME ALGORITHM

Trong T. Bui
Internal Fluid Mechanics Division
NASA Lewis Research Center
Cleveland, Ohio

Reda R. Mankbadi
Lewis Research Academy
NASA Lewis Research Center
Cleveland, Ohio

ABSTRACT

Numerical simulation of a very small amplitude acoustic wave interacting with a shock wave in a quasi-1D convergent-divergent nozzle is performed using an unstructured finite volume algorithm with piece-wise linear, least square reconstruction, Roe flux difference splitting, and second-order MacCormack time marching. First, the spatial accuracy of the algorithm is evaluated for steady flows with and without the normal shock by running the simulation with a sequence of successively finer meshes. Then the accuracy of the Roe flux difference splitting near the sonic transition point is examined for different reconstruction schemes. Finally, the unsteady numerical solutions with the acoustic perturbation are presented and compared with linear theory results.

INTRODUCTION

The direct numerical simulation of very small amplitude acoustic disturbances in compressible flows with shock waves is a challenging problem for computational aeroacoustics. For a successful simulation of such flows, the numerical algorithm is required to both track the extremely small disturbances of the acoustic waves and capture the shocks accurately. In addition, the appropriate algorithm needs to be simple and efficient so that it can be used in simulations of flows with complex geometries.

For the simulation of flows with complex geometries, unstructured finite volume methods have proven to be very popular, and simulations of a large number of flows have been done with good results using this approach. However, most of the finite volume simulations to date were done for steady flows, and it is not clear that unstructured finite volume algorithms can accurately capture both the acoustic wave and the shock simultaneously in a computation. Therefore, there is a need to assess the accuracy of these methods for acoustic calculations.

In this paper, we perform numerical simulations of very small amplitude acoustic waves incident on supersonic and transonic flows in a quasi-1D convergent-divergent nozzle using an unstructured finite volume algorithm with piece-wise linear, least square reconstruction, Roe flux difference splitting, and second-order MacCormack time marching. First, the spatial accuracy of the algorithm is evaluated for steady flows with and without the normal shock by running the simulation with a sequence of successively finer meshes. Then the accuracy of the Roe flux difference splitting near the sonic transition point is investigated for different reconstruction schemes. Finally, the unsteady numerical solutions with the acoustic perturbation are presented and compared with linear theory results.

TEST CASE DESCRIPTION

The test case category 5 from the 1994 ICASE/LaRC Workshop on Benchmark Problems in Computational Aeroacoustics was selected for this study. This test case consists of a very small amplitude acoustic wave superimposed on the steady flow in a quasi-1D convergent-divergent nozzle. The amplitude of the wave is specified to be in the order of 10^{-6} times the dynamic pressure based on the speed of sound of the incoming flow.

The nozzle geometry is shown in fig. 1. The nozzle dimensions, flow conditions, and normalizing conditions are the same as those specified in the ICASE/LaRC workshop. To establish the normal shock in the nozzle, the exit pressure to inlet total pressure ratio was specified to be 0.76. The case with the normal shock is similar to the study done by Meadows et al. (1993) using the MacCormack and higher-order ENO schemes. In the current study, the inlet Mach number is 0.5, and the exit Mach number is 1.55 (without shock) or 0.6 (with shock).

Since the test case is quasi-1D, the computational grid used is identical to the one that would be used in a calculation with a structured algorithm. However, the numerical algorithm used here is

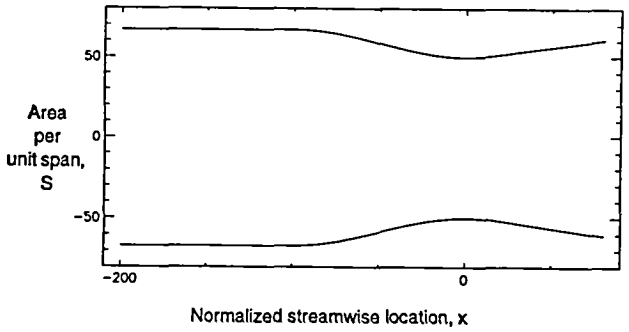

Fig. 1 Nozzle geometry

unstructured, and a simple test case such as this will allow efficient and thorough evaluation of the algorithm's accuracy.

NUMERICAL PROCEDURE

The governing equation used for this study is the quasi-1D Euler equation in the following form:

$$\frac{\partial U}{\partial t} + \frac{\partial F}{\partial x} = Q \tag{1}$$

where

$$U = \begin{bmatrix} \rho \\ \rho u \\ E_t \end{bmatrix} \qquad F = \begin{bmatrix} \rho u \\ \rho u^2 + P \\ (E_t + P)\,u \end{bmatrix} \qquad Q = \begin{bmatrix} -\frac{1}{S}\frac{\partial S}{\partial x}\rho u \\ -\frac{1}{S}\frac{\partial S}{\partial x}\rho u^2 \\ -\frac{1}{S}\frac{\partial S}{\partial x}(E_t + P)\,u \end{bmatrix} \tag{2}$$

The above equation is discretized using the finite volume approach. In this approach, eq. (1) is integrated over a finite volume which reduces to a single strip of length Δx for the 1D case. The major steps in the solution procedure are: (1) reconstruction, (2) flux computation, and (3) evolution. This is a standard finite volume solution procedure that has been used in previous works, and it is described in detail by Barth (1993).

Step 1: Reconstruction - A cell-centered scheme is used here. The piece-wise linear, least square reconstruction procedure used in this study is similar to those used by Barth (1993) and Coirier (1994). Each of the three conservation variables is assumed to vary linearly within a finite volume as:

$$U(x) = \bar{U} + \phi U_x (x - \bar{x}) \tag{3}$$

The overbars in eq. (3) denote cell-averaged values, and ϕ is a gradient limiter, described by Barth (1993). The gradient limiter is needed so that the reconstruction polynomial, eq. (3), does not produce new extrema that are outside the range of the cell-averaged data used in the reconstruction process. A different gradient limiter is used for each of the three conservation variables. Note that the cell-averaged value of the unknown is recovered when eq. (3) is integrated over the finite volume.

$\bar{U}$ is updated in step 3 below. Following Coirier (1994), U_x is computed using a least square procedure that minimizes the differences between the cell averages of the reconstructed polynomial and the cell averages of the support set. For this 1D problem, the support set consists of the left and right neighboring cells, and U_x is computed as:

$$U_x = \frac{\sum \bar{U}_i (\bar{x}_i - \bar{x}) - \bar{U} \sum (\bar{x}_i - \bar{x})}{\sum (\bar{x}_i - \bar{x})^2} \tag{4}$$

Where the i index denotes the left and right neighboring cells.

Step 2: Flux computation - With a piece-wise linear reconstruction of the solution unknowns, the conservation variables are continuous and assumed to vary linearly within a finite volume. However, there is no guarantee that they will be continuous across adjacent volumes, since a different linear function is used in each volume. As the result, a flux formula is needed to compute a single flux at a finite volume boundary given fluxes from the adjacent volumes. A popular flux formula used in finite volume codes is the Roe flux difference splitting, and it is used here.

Step 3: Evolution - A large number of time marching algorithms is available to advance the solution unknowns in time. Since the problem is unsteady, an accurate time marching algorithm is desired. In the current work, the two-stage, second-order MacCormack time marching algorithm is used because of its simplicity. A CFL number of 0.9 based on the minimum Δx and maximum (u+a) is used in all computations, where u and a are the local flow speed and speed of sound, respectively.

BOUNDARY CONDITIONS

Boundary conditions are needed to update the incoming flux that is going into the first finite volume at the nozzle inlet and the outgoing flux that is passing out of the last volume at the exit. Accurate boundary condition implementations are important for successful simulations of flows with unsteady, acoustic perturbations. For the nozzle problem under consideration, the inflow boundary conditions should accurately specify the inflow conditions and the incoming acoustic wave, and the outflow boundary conditions must allow the outgoing perturbations to pass without introducing non-physical reflections back into the computational domain.

Different boundary condition implementations were tried, and an implementation that gave the best results is described below.

Inflow - The incoming flow is always subsonic for this test case, so the boundary conditions used are:

1. Specified P_{tot}
2. Specified T_{tot}
3. $\frac{\partial P}{\partial t} - \rho c \frac{\partial u}{\partial t} = -(u - c)\left(\frac{\partial P}{\partial x} - \rho c \frac{\partial u}{\partial x}\right)$

The outgoing compatibility relation 3 above is solved with $\frac{\partial P}{\partial x}$ and $\frac{\partial u}{\partial x}$ discretized using information from the computational

domain. For the acoustic computations, P_{tot} and T_{tot} are specified as functions of time.

Outflow - The outgoing flow is supersonic for the case with no shock and subsonic for the case with shock. The applicable compatibility relations are:

1. $\frac{\partial \rho}{\partial t} - \frac{1}{c^2}\frac{\partial P}{\partial t} = -u\left(\frac{\partial \rho}{\partial x} - \frac{1}{c^2}\frac{\partial P}{\partial x}\right)$

2. $\frac{\partial P}{\partial t} + \rho c\frac{\partial u}{\partial t} = -(u+c)\left(\frac{\partial P}{\partial x} + \rho c\frac{\partial u}{\partial x}\right) - \frac{1}{S}\frac{\partial S}{\partial x}\rho u c^2$

3. $\frac{\partial P}{\partial t} - \rho c\frac{\partial u}{\partial t} = -(u-c)\left(\frac{\partial P}{\partial x} - \rho c\frac{\partial u}{\partial x}\right) - \frac{1}{S}\frac{\partial S}{\partial x}\rho u c^2$

If the outflow is supersonic, then compatibility relations 1,2, and 3 are solved.

If the outflow is subsonic, then compatibility relations 1 and 2 are solved and the nozzle exit pressure is specified.

If the outflow is subsonic with acoustic perturbations, then compatibility relations 1 and 2 are solved together with a modified equation instead of the compatibility relation 3. The modified equation used is:

$$\frac{\partial P}{\partial t} - \rho c\frac{\partial u}{\partial t} = 0$$

RESULTS AND DISCUSSIONS

All computations are done on an IBM RS 6000 workstation using double precision (64 bit) floating point arithmetic. Converged steady flow solutions are obtained to machine precision. At convergence, the residual values typically have decreased by about 14 orders of magnitude. The acoustic computations are started from the converged steady flow solutions. To assess the spatial accuracy of the method for steady flows with and without the normal shock, computations are performed with a sequence of successively finer meshes. Log-log plots of the L_1 norm of the error versus the number of mesh points are made, and the spatial order of accuracy of the method can be obtained from the slopes of these plots. From fig. 2, the spatial order of accuracy is seen to be better than two for the case with no shock and between one and two for the case with the normal shock. This is to be expected, since the limiters used in this algorithm essentially reduce the order of accuracy down to one in the neighborhood of a flow discontinuity.

For steady flows, Roe flux difference splitting (FDS) has been found to give non-physical expansion shocks at the sonic transition points. Since this would adversely affect the unsteady calculations, it was explored further with a 30-cell grid. Fig. 3 shows that with a piece-wise constant reconstruction, expansion shocks in the numerical solutions cause them to depart significantly from the exact solutions. However, with the piece-wise linear, least square reconstruction, there is no expansion shock, and the numerical solutions interpolate the exact solutions almost exactly.

A close examination of the results in fig. 3 reveals that with the 30-cell grid used, the sonic transition point at the throat of the nozzle is inside a cell. When the piece-wise linear reconstruction is used, the Roe FDS never really see the sonic transition point, so that a fortuitous choice of grid might have helped eliminating the expansion shocks in the piece-wise linear calculations.

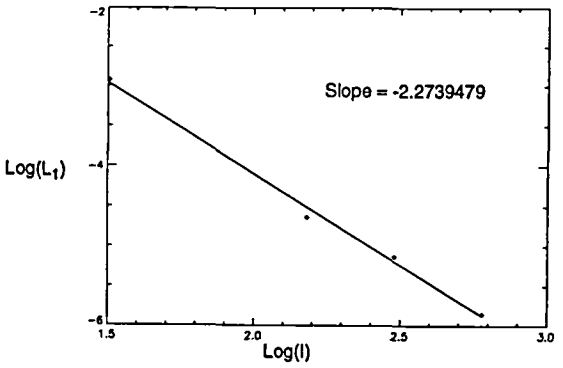

a. Steady flow with no shock

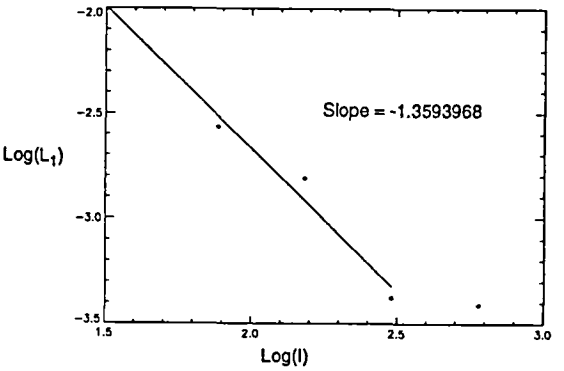

b. Steady flow with shock

Fig. 2 L_1 norm of the error vs. number of grid points, I

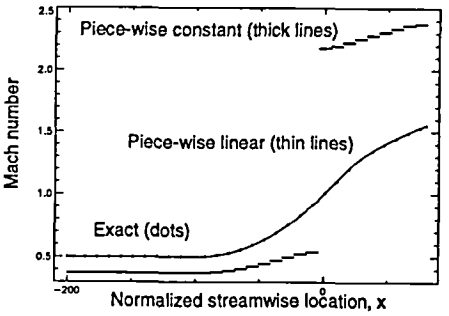

a. Steady flow with no shock

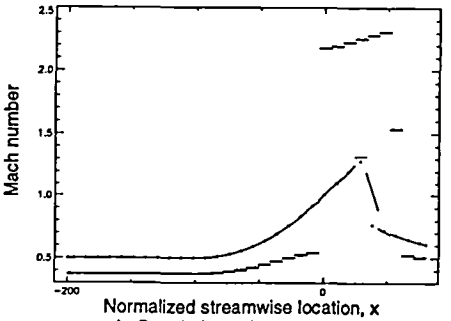

b. Steady flow with shock

Fig. 3 Comparison of piece-wise constant and piece-wise linear steady flow results

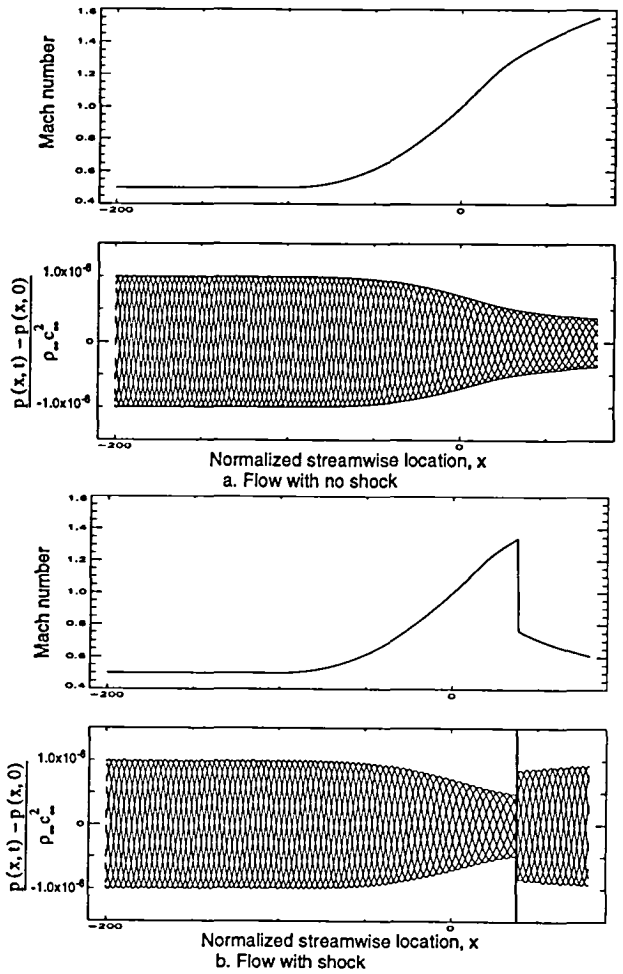

Fig. 4 Fine grid solutions with 1200 cells

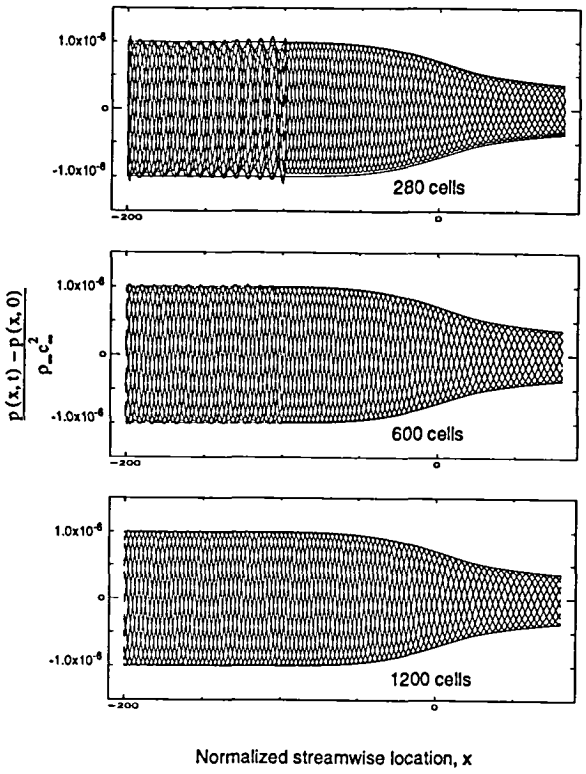

Fig. 5 Grid refinement study, no shock case

To see if that is the case, a 28-cell grid was constructed so that the sonic transition point is located exactly at a cell boundary where the Roe FDS is applied. The numerical solution obtained using this grid is essentially the same as the 30-cell grid solution, so it appears that when piece-wise linear, least square reconstruction is used with Roe FDS, an entropy fix is not necessary to eliminate the expansion shocks.

Fig. 4 shows the fine grid numerical results with 1200 cells. Results for the case with no shock are shown in 4a, and those for the case with shock are shown in 4b. It can be seen in fig. 4b that the normal shock is sharply captured by this numerical algorithm with no visible pre- or post-shock oscillations. The computed Mach number distributions of the steady flows agree almost exactly with the analytical solutions. The acoustic pressure perturbations throughout the entire computational domain are also plotted in fig. 4. In these plots, snapshots of pressure perturbations due to the acoustic wave in the nozzle at different times are superimposed on the same plot.

Fig. 5 shows the results of the grid refinement study for the no shock case. In this case, the exit Mach number is supersonic, and there is no shock in the nozzle. For the case with 280 cells (corresponding to about 30 cells per wave length), it can be seen that there are some spurious pressure oscillations near the nozzle inlet. In Aftosmis et al. (1994), it was found that the piece-wise linear reconstruction with the Barth's limiter can produce spurious pressure oscillations in their numerical simulation of the supersonic vortex, and a similar thing might be happening here. These oscillations are visibly reduced when a finer mesh of 600 cells was used, and they are essentially eliminated for a mesh of 1200 cells. This is to be expected, since the action of the limiters diminishes with finer meshes.

Grid refinement results for the case with the normal shock is shown in fig. 6. In this case, there is a normal shock located downstream of the nozzle throat, and the acoustic pressure perturbation is amplified across the shock wave. For the mesh of 300 cells, the computed jump in pressure perturbation is about 6% higher than the linear theory prediction used by Meadows et al. (1993). When the mesh is refined to 1200 cells, the difference between computational and linear theory predictions is reduced to about 1%.

Finally, fig. 7 plots the time history of the exit pressure for all of the cases considered for one period of the acoustic wave. For the no shock case, the result using a fourth-order accurate method obtained by Casper (1994) with a 280-point mesh is also plotted for the purpose of comparison. It can be seen that the coarser mesh solutions have a small phase error, which can be eliminated using a finer mesh.

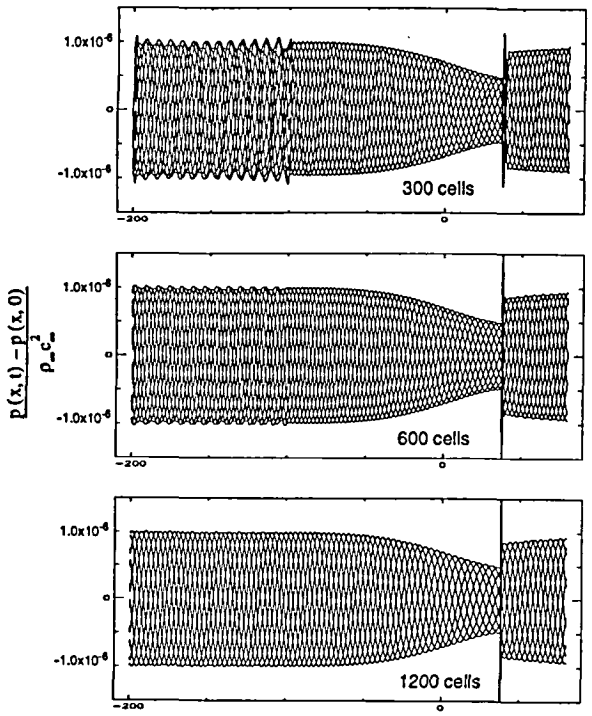

Fig. 6 Grid refinement study, with shock case

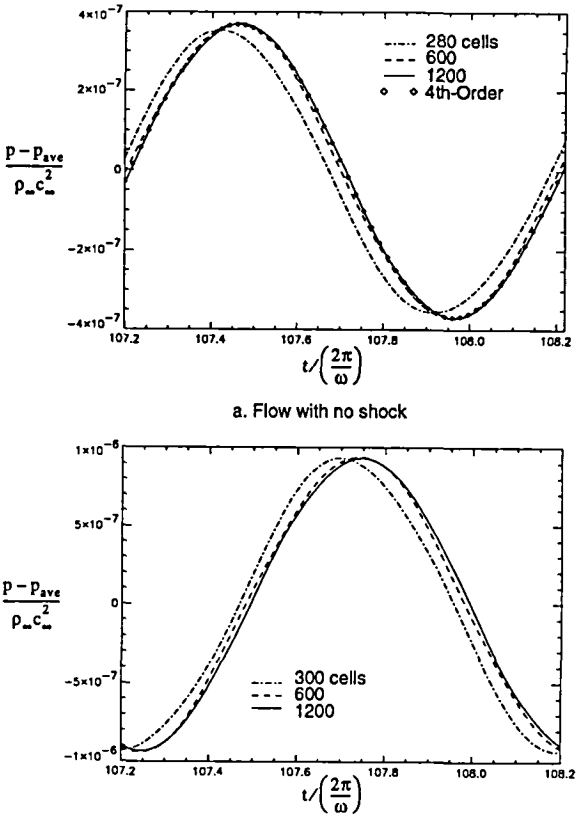

Fig. 7 Time history of the nozzle exit pressure with the acoustic perturbation

CONCLUSIONS

Direct numerical simulation of acoustic waves incident on compressible flows with and without a normal shock inside a quasi-1D convergent-divergent nozzle was performed using an unstructured finite volume algorithm with piece-wise linear, least square reconstruction, Roe flux difference splitting, and second-order MacCormack time marching. For steady flows, the agreement between the numerical method and the exact solution was very good. The spatial order of accuracy of the above method was found to be better than two for the no shock case, and between one and two for the case with the normal shock. With the piece-wise linear, least square reconstruction, the Roe FDS was found to give the physically correct solution without using an entropy fix. The above method was able to both track the propagation of a very small amplitude acoustic wave and capture the shock wave accurately.

REFERENCES

Aftosmis, M., Gaitonde, D., and Tavares T. S., "On the accuracy, Stability and Monotonicity of Various Reconstruction Algorithms for Unstructured Meshes," AIAA paper 94-0415, Jan. 1994.

Barth, T. J., "Recent Developments in High Order K-Exact Reconstruction on Unstructured Meshes," AIAA Paper 93-0668, Jan. 1993.

Casper, J., Category 5 problem, ICASE/LaRC Workshop on Benchmark Problems in Computational Aeroacoustics, Hampton, VA, October 24-26, 1994. (To be published in a NASA CP)

Coirier, W. J., "An Adaptively-Refined, Cartesian, Cell-Based Scheme for the Euler and Navier-Stokes Equations," NASA TM 106754, Oct. 1994.

Meadows, K. R., Casper, J., and Caughey, D. A., "A Numerical Investigation of Sound Amplification by a Shock Wave," FED-Vol. 147, Computational Aero- and Hydro-Acoustics, ASME 1993, pp. 47-52.

REPORT DOCUMENTATION PAGE

Form Approved
OMB No. 0704-0188

1. AGENCY USE ONLY (*Leave blank*)	2. REPORT DATE	3. REPORT TYPE AND DATES COVERED
	September 1995	Technical Memorandum

4. TITLE AND SUBTITLE

Direct Numerical Simulation of Acoustic Waves Interacting With a Shock Wave in a Quasi-1D Convergent-Divergent Nozzle Using an Unstructured Finite Volume Algorithm

5. FUNDING NUMBERS

WU-505-62-52

6. AUTHOR(S)

Trong T. Bui and Reda R. Mankbadi

7. PERFORMING ORGANIZATION NAME(S) AND ADDRESS(ES)

National Aeronautics and Space Administration
Lewis Research Center
Cleveland, Ohio 44135-3191

8. PERFORMING ORGANIZATION REPORT NUMBER

E-9934

9. SPONSORING/MONITORING AGENCY NAME(S) AND ADDRESS(ES)

National Aeronautics and Space Administration
Washington, D.C. 20546-0001

10. SPONSORING/MONITORING AGENCY REPORT NUMBER

NASA TM-107070

11. SUPPLEMENTARY NOTES

Prepared for the Joint Fluids Engineering Conference cosponsored by the American Society of Mechanical Engineers and the Japan Society of Mechanical Engineers, Hilton Head, South Carolina, August 13-18, 1995. Responsible person, Trong T. Bui, organization code 2660, (216) 433-5639.

12a. DISTRIBUTION/AVAILABILITY STATEMENT

Unclassified - Unlimited
Subject Categories 02, 64, and 71

This publication is available from the NASA Center for Aerospace Information, (301) 621-0390.

12b. DISTRIBUTION CODE

13. ABSTRACT (*Maximum 200 words*)

Numerical simulation of a very small amplitude acoustic wave interacting with a shock wave in a quasi-1D convergent-divergent nozzle is performed using an unstructured finite volume algorithm with piece-wise linear, least square reconstruction, Roe flux difference splitting, and second-order MacCormack time marching. First, the spatial accuracy of the algorithm is evaluated for steady flows with and without the normal shock by running the simulation with a sequence of successively finer meshes. Then the accuracy of the Roe flux difference splitting near the sonic transition point is examined for different reconstruction schemes. Finally, the unsteady numerical solutions with the acoustic perturbation are presented and compared with linear theory results.

14. SUBJECT TERMS	15. NUMBER OF PAGES
Aeroacoustics; Unstructured algorithm; Compressible flows	07
	16. PRICE CODE: A02

17. SECURITY CLASSIFICATION OF REPORT	18. SECURITY CLASSIFICATION OF THIS PAGE	19. SECURITY CLASSIFICATION OF ABSTRACT	20. LIMITATION OF ABSTRACT
Unclassified	Unclassified	Unclassified	